Laser and Particle Beams (2017), *35*, 513–519.

doi:10.1017/S0263034617000519

Departure from MHD prescriptions in shock formation over a guiding magnetic field

A. BRET,[1,2] A. PE'ER,[3] L. SIRONI,[4] M.E. DIECKMANN,[5] AND R. NARAYAN[6]

[1]ETSI Industriales, Universidad de Castilla-La Mancha, 13071 Ciudad Real, Spain
[2]Instituto de Investigaciones Energéticas y Aplicaciones Industriales, Campus Universitario de Ciudad Real, 13071 Ciudad Real, Spain
[3]Physics Department, University College Cork, Cork, Ireland
[4]Department of Astronomy, Columbia University, New York, NY 10027, USA
[5]Department of Science and Technology, Linköping University, SE-60174 Norrköping, Sweden
[6]Harvard-Smithsonian Center for Astrophysics, 60 Garden Street, MS-51 Cambridge, MA 02138, USA

(RECEIVED 8 May 2017; ACCEPTED 21 June 2017)

Abstract

In plasmas where the mean-free-path is much larger than the size of the system, shock waves can arise with a front much shorter than the mean-free-path. These so-called "collisionless shocks" are mediated by collective plasma interactions. Studies conducted so far on these shocks found that although binary collisions are absent, the distribution functions are thermalized downstream by scattering on the fields, so that magnetohydrodynamics prescriptions may apply. Here we show a clear departure from this pattern in the case of Weibel shocks forming over a flow-aligned magnetic field. A micro-physical analysis of the particle motion in the Weibel filaments shows how they become unable to trap the flow in the presence of too strong a field, inhibiting the mechanism of shock formation. Particle-in-cell simulations confirm these results.

Keywords: Collisionless shocks; MHD; Weibel instability

1. INTRODUCTION

In a fluid where the mean-free-path is small compared with the dimensions of the system, the front of a shock wave is a few mean-free-paths thick (Zel'dovich & Raizer, 2002). As such, it is treated as a discontinuity in the fluid limit. In plasmas where the mean-free-path is much larger than the characteristic lengths involved, shock waves can also develop, with a front much smaller than the mean-free-path (Petschek, 1958; Sagdeev, 1966). Such shocks have been dubbed "collisionless shocks". While their very existence was still under debate in the 1980s (Sagdeev & Kennel, 1991), *in-situ* measurements of the earth bow shock have definitively confirmed they do exist, as its front is about 100 km thick, while the proton mean-free-path at this location is comparable with the Sun–Earth distance (Bale *et al*., 2003; Schwartz *et al*., 2011).

Being electromagnetic objects, the formation of these shocks from the encounter of two plasma shells, vastly differs according to the initial energy of the collision, or the presence and orientation of an external magnetic field (Treumann, 2009; Stockem *et al*., 2014). When two electron/ion plasmas collide for example, each one displays a Debye sheath at its border (Gurnett & Bhattacharjee, 2005), with a potential jump $\sim k_B T_e/q$ high, where T_e is the electronic temperature and q is the elementary charge. If the kinetic energy of the shells is smaller than this potential jump, the formation is mediated by the interaction of the Debye sheaths, and an electrostatic shock follows (Stockem *et al*., 2014). At higher energies, the shells easily overcome the Debye sheaths, and the formation is mediated by the counter-streaming instabilities, which grow when the two shells overlap (Stockem Novo *et al*., 2015; Ruyer *et al*., 2017).

Note that electrostatic shocks have already been produced in laboratory (Yuan *et al*., 2017). Weibel-type shocks should require NIF-type installations. As such, they have not been produced yet, although experiments are scheduled in the near term (Park *et al*., 2016). The present paper focuses on the second case, namely, high-energy collisions.

Consider, to simplify even further, the encounter of two identical, cold, pair plasmas. Being made up of particles of identical masses, they do not display any Debye sheaths at

Address correspondence and reprint requests to: A. Bret, ETSI Industriales, Universidad de Castilla-La Mancha, 13071 Ciudad Real, Spain and Instituto de Investigaciones Energéticas y Aplicaciones Industriales, Campus Universitario de Ciudad Real, 13071 Ciudad Real, Spain. E-mail: antoineclaude.bret@uclm.es

their border. If their initial velocity is relativistic, then the Weibel instability is the fastest growing one when the two shells overlap (Bret *et al.*, 2010; Bret, 2016*a*). This instability generates magnetic filaments, which may be able to block the flow that keeps entering the overlapping region (Bret, 2015*a*, *b*).

Note that at least in pair plasmas, the formation process in the non-relativistic regime follows the same pattern (Dieckmann & Bret, 2017). Here the absence of Debye sheaths allows the two shells to overlap, regardless of their initial kinetic energy. Because the Weibel instability eventually relies on the Lorentz force repelling opposite currents (Bret, 2012), its growth rate vanishes in the limit of zero counter-streaming velocity, and the two-stream instability takes the lead (Bret, 2016*a*). The two-stream instability grows, saturates, and generates enough turbulence to block the incoming flow, and build-up the shock (Dieckmann & Bret, 2017).

When a collisionless shock does form, it fulfills the Rankine–Hugoniot (RH) jump conditions to a very good approximation. The agreement is not perfect though, because particles reflected at the front, or accelerated, escape the RH budget (Stockem *et al.*, 2012; Bret, 2015*a*, *b*). Yet, it was thought until recently that magnetohydrodynamics (MHD) was a good guide for the shock properties, even in the collisionless regime. The aim of this paper is to explain when microphysics allows for the fulfillment of the MHD prescriptions, and when it does not.

Section 2 is devoted to the analysis of particles' trajectories in the Weibel filaments, when no external magnetic field is present. In accordance with particle-in-cell (PIC) simulations, such analysis concludes that a shock always forms for the simple system considered. Section 3 briefly reviews the MHD expectations for the kind of system treated here. Section 4 then explains how a flow-aligned magnetic field can hinder shock formation, even though such a field is perfectly decoupled from the fluid in the MHD approximation. Finally, Section 5 presents a series of PIC simulations confirming the analysis conducted in Section 4.

2. SHOCK FORMATION AND PARTICLE MOTION IN UNMAGNETIZED WEIBEL FILAMENTS

Let us start treating the unmagnetized case first. The two plasma shells have initial densities n_0, velocities $\pm v_0 \mathbf{e}_z$ and common Lorentz factor $\gamma_0 = (1-\beta_0^2)^{-1/2}$, with $\beta_0 = v_0/c$.

Here the plasma shells overlap and the overlapping region turns unstable. While many instabilities grow, the Weibel one is the fastest in the relativistic regime (Bret *et al.*, 2010; Bret, 2016*a*). Choosing z as the axis of the flow (see Fig. 1) the Weibel instability grows with growth rate δ_W and develops at saturation a field which reads

$$\mathbf{B}_W = B_f \sin kx\, \mathbf{e}_y, \tag{1}$$

where k is the fastest growing wave mode and B_f the amplitude of the Weibel field at saturation. At this stage, we can

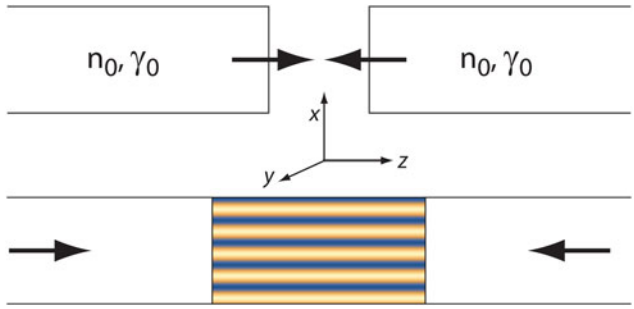

Fig. 1. System considered. Two identical pair plasma shells run toward each other. As they overlap, the overlapping region turns unstable to the Weibel instability. At saturation, this instability generates the magnetic filaments, which are schematically represented on the bottom figure.

therefore schematically model the system by the three regions represented in Figure 1-bottom. The left/right regions where the flow keeps streaming rightward/leftward, and the central region where stands the field describes by Eq. (1).

Working in the test particle approximation, the trajectory of particles entering this region can be analyzed numerically. Assume one of them is injected at $x = x_0$ with velocity $\mathbf{v} = v_0 \mathbf{e}_z$. Proceeding to the following change of variables:

$$\mathbf{X} = k\mathbf{x},\ \tau = t\omega_{B_f} \quad \text{with} \quad \omega_{B_f} = \frac{qB_f}{\gamma_0 mc}, \tag{2}$$

the equations of motion read

$$\ddot{X} = -\dot{Z} \sin X, \tag{3}$$

$$\ddot{Y} = 0, \tag{4}$$

$$\ddot{Z} = \dot{X} \sin X \tag{5}$$

with initial conditions

$$\mathbf{X}(\tau = 0) = (kx_0, 0, 0), \tag{6}$$

$$\dot{\mathbf{X}}(\tau = 0) = \left(0, 0, \frac{kv_0}{\omega_{B_f}}\right). \tag{7}$$

The symmetries of the problem allow one to restrict the analysis to $X \in [0,\ \pi]$ (Bret, 2015*a*, *b*).

The analytical/numerical determination of the region of the phase-space parameters $(X_0, \dot{Z}_0)$ where the test particle does not stream through the filaments results in the shaded region in Figure 2. It turns out that regardless of its initial position and velocity, a particle entering the filaments keeps streaming through it if,

$$k^{-1} < \frac{v_0}{\omega_{B_f}}, \tag{8}$$

https://doi.org/10.1017/S0263034617000519 Published online by Cambridge University Press

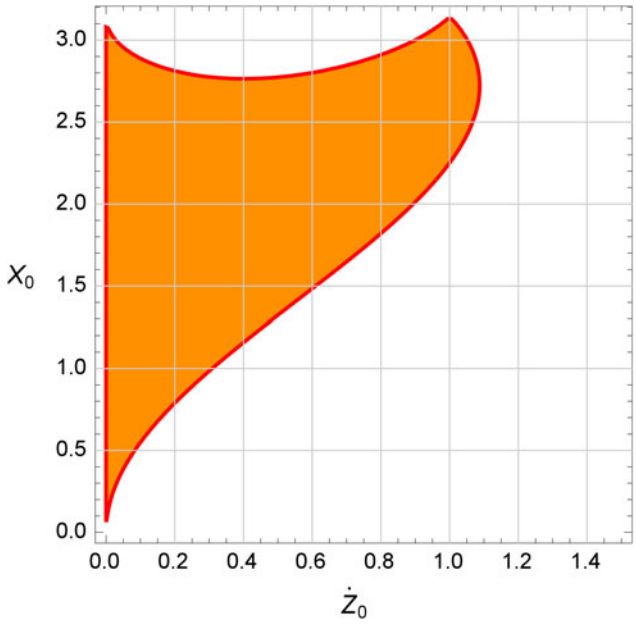

Fig. 2. Whenever a particle in injected into the Weibel filaments with initial conditions out of the shaded area, it keeps streaming through the filaments.

which simply states that the Larmor radius in the peak field is larger than k^{-1}, the coherence length of the Weibel field. On the contrary, that is, if the Larmor radius is much smaller than k^{-1}, test particles are trapped in the Weibel filaments.

Since B_f can be assessed through $\omega_{B_\mathrm{f}} \sim \delta_\mathrm{W}$ (Davidson *et al.*, 1972; Grassi *et al.*, 2017), a little algebra shows that Eq. (8) is never fulfilled at saturation of the Weibel instability. In other words, the Weibel filaments at saturation are large enough to block the incoming flow. As a result, the density in the overlapping region increases until the shock forms (Bret *et al.*, 2013*a*, *b*).

Before we turn to the magnetized case, let us briefly remind the predictions of MHD for the collision of two such plasma shells.

3. MHD PREDICTIONS

Our two plasma shells are cold and collide at relativistic velocities. We thus expect a shock to be formed. For $\gamma_0 \gg 1$, and measuring all quantities in the downstream reference frame, we expect a density jump ~ 4 and a shock front velocity $\sim c/3$ (Blandford & McKee, 1976; Marcowith *et al.*, 2016; Pelletier *et al.*, 2017). Such are indeed the values consistently obtained in PIC simulations of the process. Although binary collisions are absent, the fields are capable of isotropizing the particles' distribution functions, so that MHD conclusions remain valid (Bret, 2015*a*, *b*).

How does a flow-aligned external field modify these conclusions? The key point here is that in the case of a flow-aligned field, the field and the fluid are mathematically decoupled (Lichnerowicz, 1976; Majorana & Anile, 1987). As a result, head-on collision of two plasma shells over a flow-aligned field gives, according to MHD, exactly the same shock, regardless of the field strength. The density jump at the shock front should therefore be the same.

Such are the macro-physical prescriptions: no field effects. However, these prescriptions apply insofar as particles are trapped in the overlapping region, with an isotropized distribution function. Let see now how a flow-aligned field can jeopardize this property from the microscopic level.

4. PARTICLE MOTION IN MAGNETIZED WEIBEL FILAMENTS, DEPARTURE FROM MHD PREDICTIONS

We here elaborate further on Section 2 by considering a flow-aligned field $\mathbf{B}_0$. One can expect such a "guiding" field to precisely guide the particles, making them more difficult to trap. We therefore include now an external field $\mathbf{B}_0 = B_0\,\mathbf{e}_z$ in the study. Again, the trajectory of a test particle injected in the filaments is considered. System (3) now reads (Bret, 2016*b*)

$$\ddot{X} = -\dot{Z}\sin X + \alpha\dot{Y}, \quad \text{with} \quad \alpha = B_0/B_\mathrm{f}, \tag{9}$$

$$\ddot{Y} = -\alpha\dot{X}, \tag{10}$$

$$\ddot{Z} = \dot{X}\sin X \tag{11}$$

still with initial conditions (6). The evolution of Figure 2 when the external magnetic field $\mathbf{B}_0$ increases, is pictured of Figure 3. Remarkably, beyond

$$\alpha > 1/2, \tag{12}$$

all test particles stream through the filaments, regardless of their initial position and velocity. This suggests that a strong enough flow-aligned field could jeopardize the ability of the filaments to stop the flow and initiate the shock formation. Such a behavior would therefore stand in sharp contrast with the MHD predictions.

Before we check this hypothesis with PIC simulations, we need to elaborate on the criteria (12) by expressing B_f in terms of the parameters of the problem. Here also, we consider the Weibel field reaches saturation when $\delta_\mathrm{W} = \omega_{B_\mathrm{f}}$ (Davidson *et al.*, 1972; Grassi *et al.*, 2017). In the presence of a flow-aligned magnetic field, the growth rate of the Weibel instability reads (Stockem *et al.*, 2006; Bret, 2016*a*)

$$\delta_\mathrm{W} = \omega_\mathrm{p}\sqrt{2\beta_0^2 - \sigma}, \tag{13}$$

where

$$\sigma = \frac{B_0^2/4\pi}{\gamma_0 n_0 mc^2},$$

https://doi.org/10.1017/S0263034617000519 Published online by Cambridge University Press

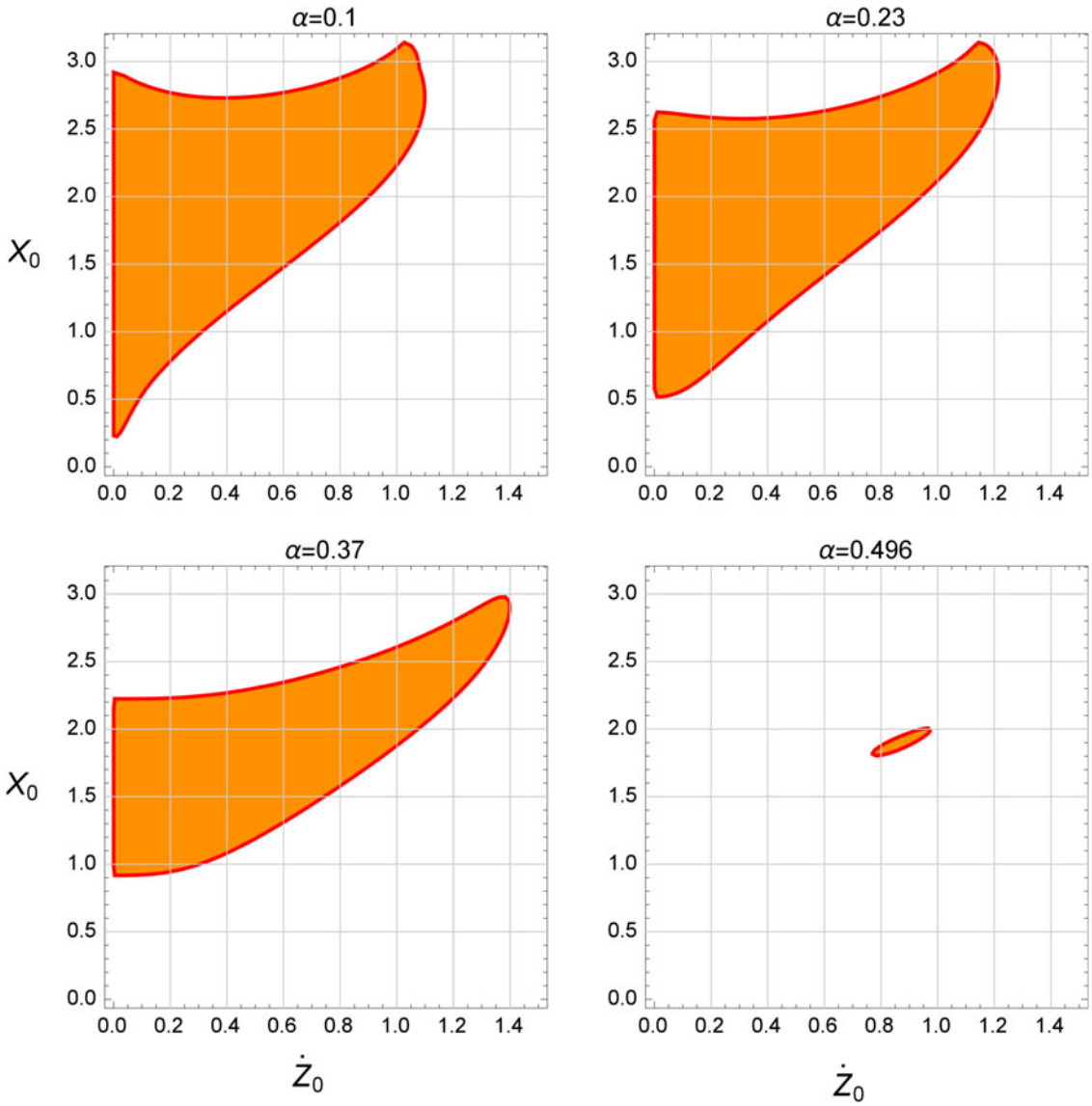

Fig. 3. Evolution of Figure 2 when the external magnetic field $\mathbf{B}_0$ measured by $\alpha = B_0/B_f$ increases. Beyond $\alpha > 1/2$, all test particles stream through the filaments, regardless of their initial position and velocity.

$$\omega_p = \sqrt{\frac{4\pi n_0 q^2}{\gamma_0 m}}. \tag{14}$$

Inserting Eq. (13) into $\delta_W = \omega_{B_f}$, we find the criteria (12) is eventually equivalent to,

$$\sigma > \frac{2}{3}. \tag{15}$$

The analysis of particle trajectories within the Weibel filaments suggests therefore that we could observe some departure from the MHD prescription beyond $\sigma = 2/3$. Let us now check it with PIC simulations.

5. PIC SIMULATIONS

We use the three-dimensional (3D) code TRISTAN-MP, which is a Massively Parallel evolution of the code TRISTAN (Buneman, 1993; Spitkovsky, 2005). The space domain simulated is 2D, while the fields and the velocities are tracked in 3D. The setup sketched in Figure 1 is simulated by the reflecting wall method, where a reflecting wall is positioned along the x-axis, at the z-position where the two shells make contact. Only the right shell is modeled. It first moves leftward, bounces back against the wall, and the bounced part interacts with the flow, which keeps flowing from the right (Spitkovsky, 2008; Dieckmann *et al.*, 2013). Each cell is initialized with 16 electrons and 16 positrons. Each cell is $c/\omega_p/10$ large, and the time step is $\Delta t = 0.045\omega_p^{-1}$.

https://doi.org/10.1017/S0263034617000519 Published online by Cambridge University Press

The initial Lorentz factor is set to $\gamma_0 = 10$, and we scan the σ-window $0 < \sigma < 3$. Some simulations have been run with $\gamma_0 = 30$, showing the same effects, as expected from criteria (15). Figure 4-top shows the density profiles of the system at time $t = 450\omega_p^{-1}$. At low magnetization, say $\sigma < 0.6$, a shock if already formed, with a density jump ~ 4 in accordance with the RH jump conditions. Yet, as magnetization increases, the "downstream" density steadily departs from the MHD predictions. As expected from the analysis performed in Section 4, the shock formation is hindered by the guiding field.

Could it be that $t = 450\omega_p^{-1}$ is too short a time for the shock to form at high σ's? Previous works on shock formation found that the formation process takes a few tens of δ_W^{-1} (Bret *et al.*, 2014, 2016). In the present case, this translates to $\sim 30\omega_p^{-1}$, at most. The snapshots in Figure 4-top are thus taken long after the expected shock formation time.

In order to further check the observed departure from MHD prescriptions, Figure 4-bottom shows the same profile at time $t = 3600\omega_p^{-1}$. Again, while a MHD-type shock has been formed and propagates for small σ's, the MHD departure is confirmed for large ones. Noteworthy, the width of the density jump dramatically increases with σ. At low magnetization, when the MHD shock is formed, the front is about $\sim 70c/\omega_p$ thick. In contrast, the transition from the upstream to the "downstream" for $\sigma = 3$ reaches $\sim 3000c/\omega_p$. In the respect, "density gradient" seems more appropriate than "density jump" to describe the density profile.

If the "downstream" were isotropized, the MHD equations would apply. We can therefore expect an increasing deviation from isotropy in the downstream at high magnetization, when a departure from the MHD prescriptions is observed. In order to assess the isotropy of the distribution function, we compute

$$\varphi = \frac{\mathrm{Var}(p_y) + \mathrm{Var}(p_z)}{2\mathrm{Var}(p_x)}, \tag{16}$$

where $\mathrm{Var}(x)$ is the statistical variance of the variable x. This quantify when measured in the reference frame of the wall, equals unity for the downstream of a formed shock, and tend to $\propto \gamma_0^{-1}$ in the far upstream (instead of 1, because of the relativistic contraction). Its value is plotted in Figure 5 at times $t = 450$ and $3600\omega_p^{-1}$. We observe what was expected: while the downstream of MHD shocks at low σ's is isotropized with $\varphi = 1$, this part of the system is no longer so at high σ's. A closer look at the distribution function in those cases shows it retains a two beams nature, in line with the micro physics analysis conducted in Section 4.

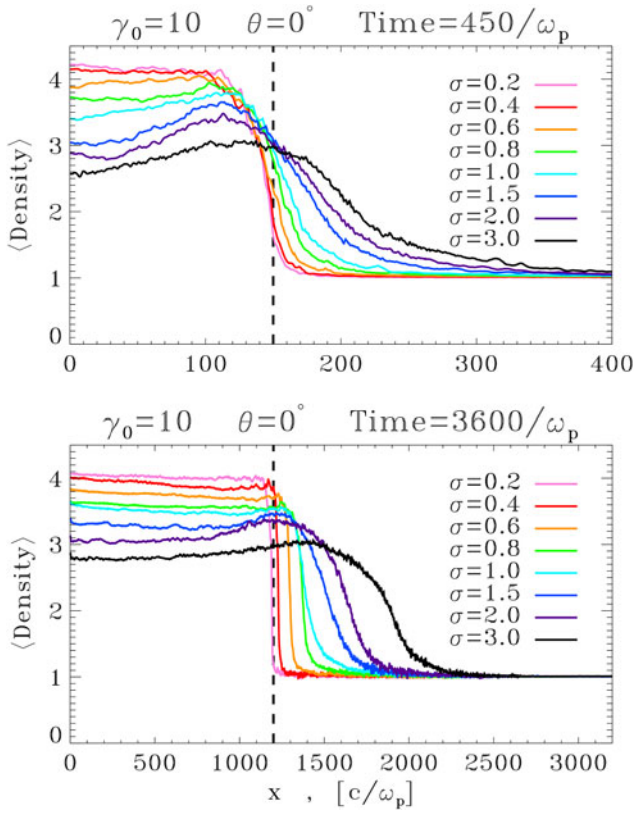

Fig. 4. PIC simulations of the process for various values of σ. The plots show the density profiles at $t = 450\omega_p^{-1}$ and $t = 3600\omega_p^{-1}$. The angle θ between the flow and the field is 0.

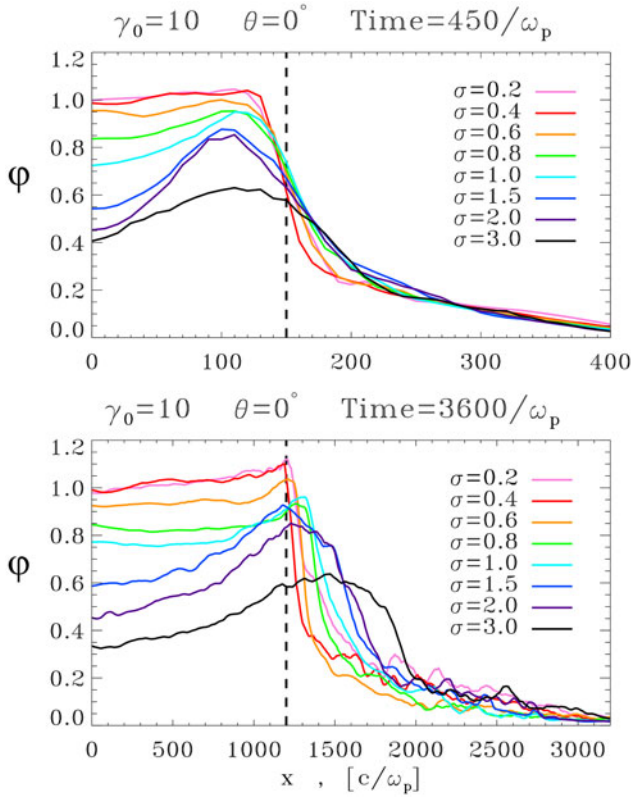

Fig. 5. Measure φ of the isotropy of the distribution function as defined by Eq. (16). At low magnetization, when a shock is formed, it equals unity in the downstream indicating an isotropic medium. At high magnetization, the downstream is not isotropized, even at late times. A closer scrutiny shows that it retains a two beams nature. The angle θ between the flow and the field is 0.

https://doi.org/10.1017/S0263034617000519 Published online by Cambridge University Press

6. CONCLUSION

In conclusion, we have found that too strong a flow-aligned magnetic field produces a significant departure from MHD expectations in shock formation, even though MHD tells such a field should not have any effects of the process. The magnetization threshold corresponds to $\sigma > 2/3$, and is independent of the initial Lorentz factor.

This departure from MHD is apparently explained by the micro-physics analysis conducted in Section 4. When the guiding field becomes too strong, particles tend to follow the field, and can no longer be trapped in the Weibel filaments. The density in the overlapping region still increases but not up to the expected density jump. The analysis of the "downstream" distribution function in that case shows it retains a two beams nature. Note also that simulations have been run tilting the field by an angle $\theta = 5^{\circ}$ in order to check the present effect is not strictly restricted to $\theta = 0^{\circ}$. Similar results have been found, evidencing the robustness of the effect.

At this junction, several questions arise:

- Is the shock formation simply delayed, or really cancelled? Does the "downstream" eventually isotropize, even at high magnetization, or does the guiding field always forbid it?
- What are the properties of these "failed shocks"? In particular, do they accelerate particles efficiently? Do they radiate?
- Is it possible to modify the MHD equations so that they render the observed micro-physics? Is it possible to express the anisotropy in terms of the field, using then modified MHD equations accounting for an anisotropic downstream (Gerbig & Schlickeiser, 2011), to retrieve the observed density jump?

These questions will be the objects of future works.

ACKNOWLEDGMENTS

A.B. acknowledges grants ENE2013-45661-C2-1-P, PEII-2014-008-P, and ANR- 14-CE33-0019 MACH. A.P. acknowledges support by the European Union Seventh Framework Program (FP7/2007-2013) under grant agreement no. 618499, and support from NASA under grant no. NNX12AO83G. R.N.'s research was supported in part by the NASA grant TCAN NNX14AB47G. O.S. acknowledges support by NASA through Einstein Post-doctoral Fellowship number PF4-150126 awarded by the Chandra X-ray Center, operated by the Smithsonian Astrophysical Observatory for NASA under contract NAS8-03060. M.E.D. acknowledges grant SNIC2015-1-305.

REFERENCES

Bale, S.D., Mozer, F.S. & Horbury, T.S. (2003). Density-transition scale at quasiperpendicular collisionless shocks. *Phys. Rev. Lett.* **91**, 265004.

Blandford, R.D. & McKee, C.F. (1976). Fluid dynamics of relativistic blast waves. *Phys. Fluids* **19**, 1130.

Bret, A. (2012). CfA Plasma Talks. *ArXiv:*1205.6259.

Bret, A. (2015*a*). Collisional behaviors of astrophysical collisionless plasmas. *J. Plasma Phys.* **81**, 455810202.

Bret, A. (2015*b*). Particles trajectories in magnetic filaments. *Phys. Plasmas* **22**, 072116.

Bret, A. (2016*a*). Hierarchy of instabilities for two counterstreaming magnetized pair beams. *Phys. Plasmas* **23**, 062122.

Bret, A. (2016*b*). Particles trajectories in Weibel magnetic filaments with a flow-aligned magnetic field. *J. Plasma Phys.* **82**, 905820403.

Bret, A., Gremillet, L. & Dieckmann, M.E. (2010). Multidimensional electron beam-plasma instabilities in the relativistic regime. *Phys. Plasmas* **17**, 120501.

Bret, A., Stockem, A., Fiúza, F., Pérez Álvaro, E., Ruyer, C., Narayan, R. & Silva, L.O. (2013*a*). The formation of a collisionless shock. *Laser Part. Beams* **31**, 487–491.

Bret, A., Stockem, A., Fiuza, F., Ruyer, C., Gremillet, L., Narayan, R. & Silva, L.O. (2013*b*). Collisionless shock formation, spontaneous electromagnetic fluctuations, and streaming instabilities. *Phys. Plasmas* **20**, 042102.

Bret, A., Stockem, A., Narayan, R. & Silva, L.O. (2014). Collisionless Weibel shocks: Full formation mechanism and timing. *Phys. Plasmas* **21**, 072301.

Bret, A., Stockem Novo, A., Narayan, R., Ruyer, C., Dieckmann, M.E. & Silva, L.O. (2016). Theory of the formation of a collisionless Weibel shock: pair vs. electron/proton plasmas. *Laser Part. Beams* **34**, 362–367.

Buneman, O. (1993). Tristan: the 3-d electromagnetic particle code. In *Computer Space Plasma Physics* (Matsumoto, H. and Omura, Y., Eds.), p. 67. Tokyo: Terra Scientific.

Davidson, R.C., Hammer, D.A., Haber, I. & Wagner, C.E. (1972). Nonlinear development of electromagnetic instabilities in anisotropic plasmas. *Phys. Fluids* **15**, 317.

Dieckmann, M.E., Ahmed, H., Sarri, G., Doria, D., Kourakis, I., Romagnani, L., Pohl, M. & Borghesi, M. (2013). Parametric study of non-relativistic electrostatic shocks and the structure of their transition layer. *Phys. Plasmas* **20**, 042111.

Dieckmann, M.E. & Bret, A. (2017). Simulation study of the formation of a non-relativistic pair shock. *J. Plasma Phys.*, **83**, 905830104.

Gerbig, D. & Schlickeiser, R. (2011). Jump conditions for relativistic magnetohydrodynamic shocks in a gyrotropic plasma. *Astrophys. J.* **733**, 32.

Grassi, A., Grech, M., Amiranoff, F., Pegoraro, F., Macchi, A. & Riconda, C. (2017). Electron Weibel instability in relativistic counterstreaming plasmas with flow-aligned external magnetic fields. *Phys. Rev. E* **95**, 023203.

Gurnett, D. & Bhattacharjee, A. (2005). *Introduction to Plasma Physics: With Space and Laboratory Applications*. Cambridge: Cambridge University Press.

Lichnerowicz, A. (1976). Shock waves in relativistic magnetohydrodynamics under general assumptions. *J. Math. Phys.* **17**, 2135–2142.

Majorana, A. & Anile, A.M. (1987). Magnetoacoustic shock waves in a relativistic gas. *Phys. Fluids* **30**, 3045–3049.

Marcowith, A., Bret, A., Bykov, A., Dieckman, M.E., Drury, L., Lembège, B., Lemoine, M., Morlino, G., Murphy, G., Pelletier, G., Plotnikov, I., Reville, B., Riquelme, M., Sironi, L. & Stockem

Novo, A. (2016). The microphysics of collisionless shock waves. *Rep. Progr. Phys.* **79**, 046901.

Park, H.-S., Ross, J.S., Huntington, C.M., Fiuza, F., Ryutov, D., Casey, D., Drake, R.P., Fiksel, G., Froula, D., Gregori, G., Kugland, N.L., Kuranz, C., Levy, M.C., Li, C.K., Meinecke, J., Morita, T., Petrasso, R., Plechaty, C., Remington, B., Sakawa, Y., Spitkovsky, A., Takabe, H. & Zylstra, A.B. (2016). Laboratory astrophysical collisionless shock experiments on Omega and NIF. *J. Phys. Conf. Ser.* **688**, 012084.

Pelletier, G., Bykov, A., Ellison, D. & Lemoine, M. (2017). Towards understanding the physics of collisionless relativistic shocks. *Space Sci. Rev.* **207**, 319–360.

Petschek, H.E. (1958). Aerodynamic dissipation. *Rev. Mod. Phys.* **30**, 966–974.

Ruyer, C., Gremillet, L., Bonnaud, G. & Riconda, C. (2017). A self-consistent analytical model for the upstream magnetic-field and ion-beam properties in Weibel-mediated collisionless shocks. *Phys. Plasmas* **24**, 041409.

Sagdeev, R. & Kennel, C. (1991). Collisionless shock waves. *Sci. Am.* (*USA*) **264**, 4.

Sagdeev, R.Z. (1966). Cooperative phenomena and shock waves in collisionless plasmas. *Rev. Plasma Phys.* **4**, 23.

Schwartz, S.J., Henley, E., Mitchell, J. & Krasnoselskikh, V. (2011). Electron temperature gradient scale at collisionless shocks. *Phys. Rev. Lett.* **107**, 215002.

Spitkovsky, A. (2005). Simulations of relativistic collisionless shocks: shock structure and particle acceleration. In *Astrophysical Sources of High Energy Particles and Radiation,* volume 801 of *American Institute of Physics Conference Series* (Bulik, T., Rudak, B. and Madejski, G., Eds.), pp. 345–350. Melville, NY: AIP.

Spitkovsky, A. (2008). On the structure of relativistic collisionless shocks in electron–ion plasmas. *Astrophys. J. Lett.* **673**, L39–L42.

Stockem, A., Fiuza, F., Bret, A., Fonseca, R. & Silva, L. (2014). Exploring the nature of collisionless shocks under laboratory conditions. *Sci. Rep.* **4**, 3934.

Stockem, A., Fiúza, F., Fonseca, R.A. & Silva, L.O. (2012). The impact of kinetic effects on the properties of relativistic electron–positron shocks. *Plasma Phys. Controll. Fusion* **54**, 125004.

Stockem, A., Lerche, I. & Schlickeiser, R. (2006). On the physical realization of two-dimensional turbulence fields in magnetized interplanetary plasmas. *Astrophys. J.* **651**, 584.

Stockem Novo, A., Bret, A., Fonseca, R.A. & Silva, L.O. (2015). Shock formation in electron-ion plasmas: mechanism and timing. *Astrophys. J. Lett.* **803**, L29.

Treumann, R.A. (2009). Fundamentals of collisionless shocks for astrophysical application, 1. Non-relativistic shocks. *Astron. Astrophys. Rev.* **17**, 409–535.

Yuan, D., Li, Y., Liu, M., Zhong, J., Zhu, B., Li, Y., Wei, H., Han, B., Pei, X., Zhao, J., Li, F., Zhang, Z., Liang, G., Wang, F., Weng, S., Li, Y., Jiang, S., Du, K., Ding, Y., Zhu, B., Zhu, J., Zhao, G. & Zhang, J. (2017). Formation and evolution of a pair of collisionless shocks in counter-streaming flows. *Sci. Rep.* **7**, 42915.

Zel'dovich, I. & Raizer, Y. (2002). *Physics of Shock Waves and High-Temperature Hydrodynamic Phenomena*. Mineola: Dover Books on Physics, Dover Publications.

https://doi.org/10.1017/S0263034617000519 Published online by Cambridge University Press